HORSERADISH PEROXIDASE COMPOUND I: EVIDENCE FOR SPIN COUPLING BETWEEN THE HEME IRON AND A 'FREE' RADICAL

C. E. SCHULZ, P. W. DEVANEY, H. WINKLER+, P. G. DEBRUNNER, N. DOAN, R. CHIANG*, R. RUTTER and L. P. HAGER

Departments of Physics and Biochemistry, University of Illinois at Urbana-Champaign, Urbana, IL 61801, USA

Received 7 May 1979

1. Introduction

In the enzymatic reaction of horseradish peroxidase (HRP) with peroxide, two intermediate complexes can be isolated, the green primary compound (I) and the red secondary compound (II) [1]. They are two and one oxidizing equivalents, respectively, above the native ferric protein, and the electronic state of the active centers in these compounds has been the subject of much speculation [2–6]. Mössbauer results are consistent with the valence state Fe^{4+} of the heme iron both in (I) and (II) [7–9]; the extra oxidizing equivalent in (I) therefore must be present as a radical. Early magnetic susceptibility measurements support a ferryl, spin $S = 1$ assignment for (II) and ferryl–radical complex for (I) [10]. On the basis of spectral similarities with oxidized porphyrin analogs (I) was modeled as a porphyrin π-cation radical with a ferryl iron [6] but this view has been disputed on the basis of NMR data [11]. ^{18}O experiments on chloroperoxidase (I) suggest oxygen as the ferryl ligand [12]. Attempts to observe the paramagnetic resonance of (I) have only met with partial success [3–5,13]. A free-radical signal was reported at $g = 1.995$, which titrated with the concentration of (I) but had an integrated intensity of only ~0.01 spins/heme [13]. Relaxation broadening by the nearby iron was suggested as a reason for the low intensity.

We present new Mössbauer and EPR data which demonstrate that:

(i) The Fe^{4+} of (I) has spin $S = 1$ and essentially the same Mössbauer parameters as (II) [9] but weakly couples to a spin $S' = 1/2$ radical;

(ii) The previously observed EPR signal of (I) [13] is but the sharp central feature of a broad spectrum, which extends over >0.2 T at 9.2 GHz and accounts for ~0.7 spins/heme;

(iii) The linewidth is due to spin coupling rather than to lifetime broadening;

(iv) At low temperatures the spin relaxation is dominated by Orbach transitions to excited doublets near 30 K.

A model Hamiltonian with an anisotropic coupling term $-\vec{S}\cdot\overleftrightarrow{J}\cdot\vec{S}'$ is proposed which is compatible with the Mössbauer and EPR data.

2. Materials and methods

HRP from Sigma was purified by the methods in [14] to an R_z-value (A_{402}:A_{280}) of 3.0. Solutions (~0.2 mM) in 0.1 M phosphate buffer (pH 6.9) were mixed in a quartz EPR tube with dilute H_2O_2 and frozen rapidly by immersion in liquid N_2. After the EPR experiments the samples were thawed, transferred to a 1 cm optical cell, diluted with buffer and rapidly scanned on a Cary 219. Concentrations of native HRP, (I) and (II) were determined from the Soret band using the extinction coefficients of [4].

+ Present address: II. Institut für Experimentalphysik, Universität Hamburg, 2000 Hamburg 50, FRG

* Present address: Grace Chemical Company, Baltimore, MD, USA

EPR data were taken on a Varian E9 X-band spectrometer with an Oxford Instruments helium flow system. Temperature readings were repeatedly checked for given flow rates against a calibrated carbon resistor in place of the sample; an accuracy of ±3% was estimated over 3–30 K.

Mössbauer experiments were done on a sample reconstituted from the apoprotein with [^{57}Fe]protoporphyrin IX. H_2O_2 was added to a 50% v/v glycerol–water solution of enriched HRP at −25°C in a 1 cm plastic cuvette. After an optical spectrum was taken with reduced pathlength the sample was frozen in liquid N_2. Mössbauer measurements were made on these plastic cells in a variable-temperature cryostat with superconducting magnet.

3. Results and discussion

The similarity in the Mössbauer parameters of (I) and (II) noted earlier for the zero-field spectra [7–9] is evident also in the high-field data (fig.1d,e). The spectra of (I) for $T > 10$ K are well reproduced by the spin Hamiltonian:

$$\mathcal{H}_S = D(S^2 - 2/3) + \beta\vec{S}\cdot\overleftrightarrow{g}\cdot\vec{H} + (\langle\vec{S}\rangle_T\cdot\overleftrightarrow{A} - \beta_n g_n\vec{H})\cdot\vec{I} + \Delta E_Q\,(3I_z^2 - I(I+1))/2I(2I-1) \quad (1)$$

with $S = 1$, $D = 32$ K and $\overleftrightarrow{g}$, $\overleftrightarrow{A}$, ΔE_Q as listed with fig.1. Equation (1) fails, however, to account for the broadening of the Mössbauer lines observed in the low-temperature, low-field spectra (fig.1a,b). This broadening arises from the interaction with the radical of spin $S' = 1/2$, and we describe the coupled system by the Hamiltonian:

$$\mathcal{H}_{S,S'} = \mathcal{H}_S + \beta\vec{H}\cdot\overleftrightarrow{g'}\cdot\vec{S'} - \vec{S}\cdot\overleftrightarrow{J}\cdot\vec{S'} \quad (2)$$

This model with a free-spin value $g' = 2$ and a weak coupling constant, $-J \simeq D/10 \simeq 3$ K, indeed yields satisfactory simulations for all fields and temperatures, (fig.1).

A complete description of the Mössbauer spectra also requires specification of the spin fluctuation rate. The model developed in [15] adapted to the spin-coupled system discussed here, shows that for all spectra of fig.1 either the fast-fluctuation limit

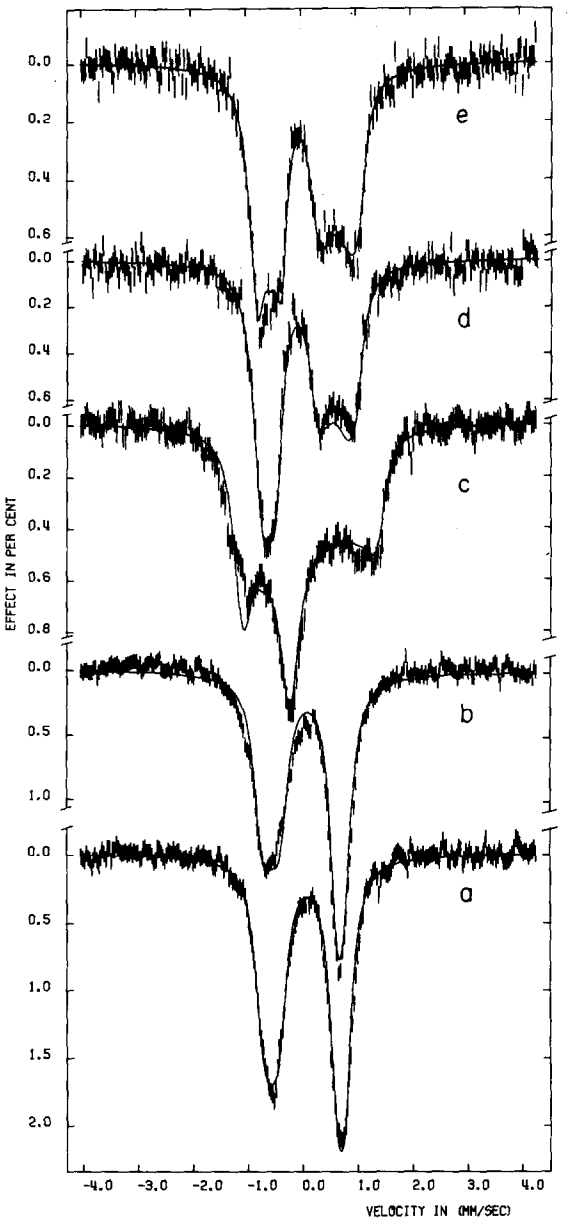

Fig.1. Mössbauer spectra of (I) under the following conditions: (a), (b) $T = 1.5$ K, $H_{\parallel} = 0.04$ T and $H_{\perp} = 0.04$ T, respectively. (c) $T = 4.2$ K, $H_{\parallel} = 5.5$ T. (d), (e) $H_{\parallel} = 3.03$ T, $T = 26$ K and 40 K, respectively. Zero velocity corresponds to the isomer shift of Fe metal at 300 K. The solid lines are simulations based on $\mathcal{H}_{S,S'}$ with the parameters $D = 32$ K, $E = 0$, $\overleftrightarrow{g} = (2.25, 2.25, 1.98)$, $g' = 2$, $\overleftrightarrow{J} = (-4,2,2)$ K, $\Delta E_Q = 1.25$ mm/s, $\eta = 0.0$, $\overleftrightarrow{A}/g_n\beta_n = (-17, -17, -6)$ T, $\delta_{Fe} = 0.08$ mm/s. Spectra (a–c) are calculated in the slow-, spectra (d) and (e) in the fast-fluctuation limit.

($T > 15$ K) or the slow-fluctuation limit ($T \leq 4.2$ K) applies.

While the spin coupling represented by eq. (2) affects the Mössbauer spectra only slightly, it radically modifies the EPR of the unpaired spin. Careful scrutiny of the weak derivative signal observed in [13] shows that it is superimposed on very broad high- and low-field wings (fig.2a). The intensity is strongly temperature dependent; the signal is lost at >30 K, but can be saturated at <5 K. For microwave powers $P \geq 60$ mW and $T \leq 3.4$ K passage conditions obtain [16,17], yielding an absorption-type spectrum (fig.2c). Numerical integration (fig.2b) of the derivative signal $d\chi''/dH$ (fig.2a) yields a spectrum in good agreement with the passage signal. Comparison of the second integral of the derivative spectrum of (I) to that of a Cu^{2+}–EDTA standard yields 0.7 ± 0.4 spins/heme.

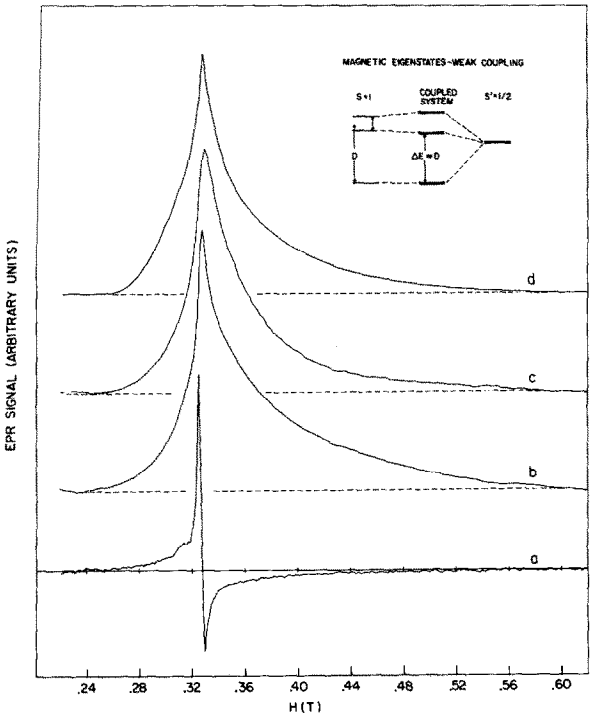

Fig.2. *X*-band EPR spectra of (I). (a) Normal slow passage derivative spectrum with $H_m = 1$ mT$_{p-p}$, $P = 0.63$ mW, $\nu_m = 10^5$ Hz. (b) Numerical integration of (a). (c) Rapid passage spectrum of (I) with $H_m = 1$ mT$_{p-p}$, $T = 3.4$ K, $P = 63$ mW, $\nu_m = 10^5$ Hz. (d) Simulation using a Gaussian distribution $p(a) = \exp(-(a-a_0)^2/2\sigma^2)$ of the exchange tensor $\overleftrightarrow{J} = a(-4,2,2)$ *K* with $a_0 = 1$ and $\sigma = 0.47$.

Evidence that the iron affects the EPR signal comes from power saturation data (fig.3) [18]. According to the Hamiltonian (eq. (2)) the eigenstates of the coupled system are 3 Kramers doublets as shown in the insert of fig.2. For weak coupling, $|J| \ll D \simeq 30$ K, the ground doublet, which gives rise to the EPR signal, is separated from the excited states by an energy $\Delta \simeq D$. Since phonon-induced transitions within a doublet are forbidden in first order, spin relaxation is dominated by Orbach processes via excited states, $T_1 \propto \exp(\Delta/T)$. This prediction is borne out by fig.3, which shows that the excited-state energy, $\Delta \simeq 29$ K, agrees well with the zero-field splitting, $D = 32$ K, deduced from Mössbauer data.

If the shape of the low-temperature EPR spectrum is not affected by lifetime broadening, it must be explained on the basis of the spin coupling tensor $\overleftrightarrow{J}$ [19], which in turn depends in a complicated way on the wavefunctions of the radical and the iron. While no explicit calculation of $\overleftrightarrow{J}$ has been performed, some constraints on its components and therefore on the geometry of the radical complex can be deduced from a simplified model. Assuming that $\overleftrightarrow{J}$ is diagonal in the frame defined by the zero-field splitting, we calculate an effective *g*-tensor for the ground state in first-order perturbation:

$$\overleftrightarrow{g}^{\mathrm{eff}}/2 - 1 = (g_x J_{xx}/D, g_y J_{yy}/D, - (J_{xx}^2 + J_{yy}^2 - g_z J_{xx} J_{yy})/2D^2) \qquad (3)$$

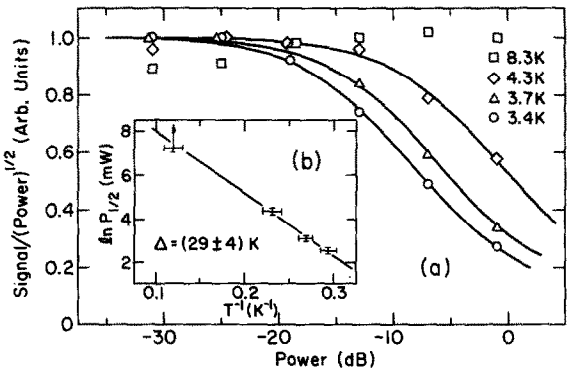

Fig.3. (a) EPR saturation data for (I) as a function of temperature. The signal *S* is taken as the peak to peak amplitude in the derivative spectrum. To avoid passage conditions $\nu_m = 10^3$ Hz was used. The solid lines are fits of $SP^{-1/2} \propto (1 + P/P_{1/2})^{-1/2}$. (b) Plot of $\ln P_{1/2}$ (fig.3a) versus T^{-1} [18].

This approximation shows that g_z^{eff} corresponds to the central peak of fig.2b,c, while the perpendicular components g_x^{eff} and g_y^{eff} correspond to the high- and low-field wings of the spectrum. It further follows that J_{xx} and J_{yy} must have comparable magnitude, but opposite sign. Within the porphyrin–radical model such a J-tensor can be realized if the z-axis is close to the heme plane, and if the dipole–dipole coupling dominates over the isotropic exchange. An estimate of the dipolar term for this model yields J_{xx} and J_{yy} of the required size, but does not rule out other geometries.

This simple model predicts EPR spectra with pronounced high- and low-field shoulders rather than smooth wings, and an exact calculation does not do much better. A satisfactory simulation is obtained, however, with a normal distribution of J-values (fig.2d). Since the dipole–dipole interaction strongly depends on distance and orientation of the moments, variations in geometry due to strain and different conformations may account for the J-spread.

In conclusion, the new Mössbauer and EPR evidence of spin coupling in (I) explains many previously puzzling observations. It is compatible with the porphyrin–radical model [6] but more work is needed before a final conclusion can be drawn.

Acknowledgements

Assistance with the high-field Mössbauer measurements by Dr E. Münck is gratefully acknowledged. Supported in part by grants PHS GM 16406, GM 07768 and NSF PCM 79-05072.

References

[1] Dunford, H. B. and Stillman, J. S. (1976) Coord. Chem. Rev. 19, 187–251.
[2] George, P. (1953) J. Biol. Chem. 201, 427–434.
[3] Brill, A. S. and Williams, R. J. P. (1961) Biochem. J. 78, 253–262.
[4] Schonbaum, G. R. and Lo, S. (1972) J. Biol. Chem. 247, 3353–3360.
[5] Peisach, J., Blumberg, W. E., Wittenberg, B. A. and Wittenberg, J. B. (1968) J. Biol. Chem. 243, 1871–1880.
[6] Dolphin, D., Forman, A., Borg, D. C., Fajer, J. and Felton, R. H. (1971) Proc. Natl. Acad. Sci. USA 68, 614–618.
[7] Maeda, Y. and Morita, Y. (1967) Biochem. Biophys. Res. Commun. 29, 680–685.
[8] Moss, T. H., Ehrenberg, A. and Bearden, A. J. (1969) Biochemistry 8, 4159–4162.
[9] Schulz, C., Chiang, R. and Debrunner, P. G. (1979) J. Physique 40, C2–534–536.
[10] Theorell, H. and Ehrenberg, A. (1952) Arch. Biochem. Biophys. 41, 442–461; report $\mu_{eff}/\mu_B = 3.45$ and 3.92 for (II) and (I), respectively, to be compared with $2\sqrt{S(S+1)} = 2.83$, $S = 1$, for (II), and $2\sqrt{S(S+1)+S'(S'+1)} = 3.32$ or $2\sqrt{(S+S')(S+S'+1)} = 3.87$, $S' = 1/2$, for (I) in weak and strong coupling, respectively.
[11] Morishima, I. and Ogawa, S. (1978) Biochemistry 17, 4384–4388.
[12] Hager, L. P., Doubek, D. L., Silverstein, R. M., Hargis, J. H. and Martin, J. C. (1972) J. Am. Chem. Soc. 94, 4363–4366.
[13] Aasa, R., Vanngard, T. and Dunford, H. B. (1975) Biochim. Biophys. Acta 391, 259–264.
[14] Shannon, L. M., Kay, E. and Lew, J. Y. (1966) J. Biol. Chem. 241, 2166–2172.
[15] Winkler, H., Schulz, C. and Debrunner, P. G. (1979) Physics Lett. 69A, 2166–2172.
[16] Weger, M. (1960) Bell Syst. Tech. J. 39, 1013–1112.
[17] The phase of the reference arm was adjusted for maximum dispersion and vanishing absorption signal. Analysis of the passage conditions at 63 mW, 3.4 K, yields Weger's case 3 [16]. $\gamma H_1^2/\omega_m H_m \simeq 0.38$ (nearly adiabatic); best guess from saturation $T_1 \simeq T_2 \simeq 10^{-6}$ s; $H_1/\omega_m H_m \sqrt{T_1 T_2} \simeq 0.08$ (rapid); $\omega_m T_1 \simeq 0.63$ (not fast); $\gamma H_1 T_1 \simeq 4.9$ (saturated). The estimated $T_2 \sim 10^{-6}$ s implies a homogeneous linewidth $\Delta H < 10^{-5}$ T.
[18] The data of fig.3 are compatible with inhomogeneous broadening, $SP^{-1/2} \propto (1 + P/P_{1/2})^{-1/2}$, and we can therefore set $P'_{1/2} \propto 1/T_1$. For an Orbach process, $T_1 \propto \exp(\Delta/T)$, a plot of $\ln P_{1/2}$ versus $1/T$ yields a straight line of slope $-\Delta$.
[19] Butler, W. F., Johnston, D. C., Okamura, M. Y., Shore, H. B. and Feher, G. (1978) Biophys. J. 21, 8a; EPR spectra of comparable width in reaction centers of photosynthetic bacteria were observed and explained by an exchange interaction between semiquinone and a high-spin Fe^{2+}.